

## Solid-State NMR and Calorimetry of Structural Waters in Helical Peptides

Maxim S. Pometun,<sup>†</sup> Usha M. Gundusharma,<sup>‡</sup> John F. Richardson,<sup>†</sup> and Richard J. Wittebort<sup>\*†</sup>

Contribution from the Department of Chemistry, University of Louisville, Louisville, Kentucky 40292, and Kimberly-Clark, Neenah, Wisconsin 54956

Received October 23, 2001

**Abstract:** The peptide hydrates Gly-Gly-Val·2H<sub>2</sub>O (GGV) and Gly-Ala-Leu·3H<sub>2</sub>O (GAL) are known to adopt  $\alpha$ -helical configurations containing waters of hydration in which each water is H-bonded to three or four peptide groups. Herein we report a thermodynamic and solid-state NMR (<sup>2</sup>H and <sup>17</sup>O) study of these peptides. From TGA and DSC, the average enthalpy per H-bond is 15 kJ/mol. The dynamics and average orientation of the hydrate are studied by powder and single-crystal <sup>2</sup>H NMR. Whereas waters that are shown by the X-ray structure to be coordinated by four hydrogen bonds do not yield observable <sup>2</sup>H NMR signals at room temperature, two of the three triply coordinated waters yield residual <sup>2</sup>H quadrupole coupling tensors characteristic of rapid 180° flip motions and the orientation of the residual tensor is that expected from the X-ray structure-derived H-bonding pattern. At -65 °C, the flip motions of triply coordinated water in GGV slow into the <sup>2</sup>H NMR intermediate exchange regime whereas the tetrahedrally coordinated water approaches the slow-exchange limit and yields an observable NMR signal. Extensive isotope exchange between water vapor and crystalline GGV establishes the presence of additional hydrate dynamics and solid-state proton transfer along a chain of water-bridged protonated  $\alpha$ -amino groups.

### Introduction

Water is a critical element in the structure and function of biomolecules. For example, when a protein folds into its native structure, hydrophobic amino acid residues are buried within the hydrophobic interior. Based on thermodynamic studies in which hydrophobic amino acids are transferred from aqueous to nonpolar media, this process is found to lead to a decrease in solvent ordering and the resultant entropy gain of the solvent is a substantial driving force in protein folding.<sup>1</sup> Consequently, the degree to which water associated with a protein is "ordered" is an important physical property. In this regard, refinement of protein structures by X-ray crystallography has advanced substantially in its treatment of the solvate structure. Early X-ray studies of proteins assumed a structureless background.<sup>2</sup> However, the identification of water positions for a substantial fraction of the total hydrate in the crystalline protein lattice is made in more recent and refined structures.<sup>3,4</sup> Complementary solid-state deuterium NMR measurements<sup>5,6</sup> indicate, however, that the lattice waters in crystalline globular proteins are highly mobile and rapidly diffuse in the lattice. The possibility of lattice

waters occupying discrete sites and rapidly jumping among them has been confirmed for hydrates of cyclodextrins<sup>7</sup> in which case the water coordinates were determined by neutron crystallography.<sup>8</sup> Moreover, solution NMR methods<sup>9</sup> show that the number of waters strongly bound to globular proteins is small compared to the number of surface waters identified in the X-ray structure. However, in cases such as fibrous proteins, water likely plays a more important structural role.<sup>3,10</sup>

Water molecules with defined hydrogen-bonded arrangements are structurally attractive in that groups otherwise too distant to form H-bond links can do so with a water bridge. However, water bridges imply an unfavorable entropic trade-off resulting from water ordering. The possibility of examining both orientational ordering and thermodynamics of "structural" waters in a simple context is made possible by small peptides that, in the solid state, fold into standard polypeptide motifs containing waters of hydration which apparently stabilize that structure.<sup>11</sup> Here we examine Gly-Gly-Val·2H<sub>2</sub>O (GGV) and Gly-Ala-Leu·3H<sub>2</sub>O (GAL). In the crystal lattice, GGV forms an extended  $\alpha$ -helix-like structure in which the C-terminal carboxylate is bridged via a water molecule, W(tet), to the protonated  $\alpha$ -amino group of the next peptide along the helix axis.<sup>12</sup> In addition,

\* Corresponding author: (e-mail) rjwitt01@athena.louisville.edu.

<sup>†</sup> University of Louisville.

<sup>‡</sup> Kimberly-Clark.

- (1) Edsall, J. T.; McKenzie, H. A. *Adv. Biophys.* **1983**, *16*, 58–183.
- (2) Finney, J. L. *Philos. Trans. R. Soc. London, Ser. B* **1977**, *278*, 3–31.
- (3) Bella, J.; Eaton, M.; Brodsky, B.; Berman, H. M. *Science* **1994**, *266*, 75–81.
- (4) Yu, B.; Blaber, M.; Gronenborn, A. M.; Clore, G. M.; Caspar, D. L. D. *Proc. Nat. Acad. Sci., U.S.A.* **1999**, *96*, 103–108.
- (5) Usha, M. G.; Wittebort, R. J. *J. Mol. Biol.* **1989**, *208*, 669–678.
- (6) Usha, M. G.; Speyer, J.; Wittebort, R. J. *Chem. Phys.* **1991**, *158*, 487–500.

- (7) Usha, M. G.; Wittebort, R. J. *J. Am. Chem. Soc.* **1992**, *114*, 1541–1548.
- (8) Betzel, C.; Saenger, W.; Hingerty, B. E.; Brown, G. *J. Am. Chem. Soc.* **1984**, *106*, 7545–7557.
- (9) Otting, G.; Liepinsh, E.; Wuthrich, K. *Science* **1991**, *254*, 974–980.
- (10) Ramachandran, G. N. In *Chemistry of Collagen*; Ramachandran, G. N., Ed.; Academic: London, 1967; Chapter 2.
- (11) Parthasarathy, R.; Chaturvedi, S.; Go, K. *Proc. Natl. Acad. Sci. U.S.A.* **1990**, *87*, 871–875.
- (12) Lalitha, V.; Subramanian, E.; Bordner, J. J. *Pept. Protein Res.* **1984**, *24*, 437–441.

W(tet) is H-bonded to the protonated  $\alpha$ -amino and carboxylate of two other neighboring, symmetry-related molecules forming an infinite chain of water-bridged protonated amino groups. A second water, W(tri), shares H-bonding with the  $\alpha$ -amino and carboxylate groups and is also linked to the Gly<sub>1</sub> carbonyl. Conformation and hydrate H-bonding in the GAL structure are closely related, but it contains a third water molecule with three H-bond partners, W'(tri).

In this study, we use solid-state  $^2\text{H}$  and  $^{17}\text{O}$  NMR to study hydrate structure and dynamics in these crystalline peptides. In addition, calorimetry is used to estimate the binding enthalpy of water in these peptides.  $^2\text{H}$  NMR is a proven technique for studying hydrate dynamics in a variety of simple compounds,<sup>5–7</sup> and it is frequently observed that a water of hydration, which appears static in the X-ray experiment, in fact undergoes rapid (rate  $>10^5 \text{ s}^{-1}$ )  $180^\circ$  flips about the 2-fold molecular axis resulting in the NMR observation of a reduced or averaged  $^2\text{H}$  electric field gradient tensor.<sup>5</sup> We use both powder and single-crystal samples grown from deuterated solvent or samples labeled by vapor-phase exchange. In situ vapor-phase exchange of the NMR sample allows characterization of water ( $^{17}\text{O}$ ) and proton ( $^2\text{H}$ ) diffusion in the crystal lattice. Compared to powder samples, the single-crystal experiment allows us to distinguish and assign the NMR signals to distinct water, amide, and  $\alpha$ -amino groups. Since the size and molecular orientation of the  $^2\text{H}$  electric field gradient tensors are approximately known, the static or average orientations of the hydrate molecules relative to the peptide are determined. This is a test of the H-bonding networks proposed on the basis of the X-ray structure. In most cases, water positions determined by X-ray methods are limited to coordinates for the oxygen atoms and the H-bonding network is based on proximity with potential donors and acceptors.

## Materials and Methods

Peptides used in this study were obtained from Bachem Bioscience Inc. Crystals were obtained by slow evaporation of solutions of the peptide in water (GGV) or water/methanol (GAL). To determine the molecular orientation of the coupling tensors, crystal faces were indexed by X-ray crystallography. GGV (dihydrate), as studied previously by X-ray methods,<sup>12</sup> crystallized in the monoclinic space group,  $P2_1$ , with cell parameters within experimental error of those previously reported.<sup>12</sup> The crystals grew as needles with the  $a$  axis along the needle and a well-developed  $ab$  face. Crystals were conveniently mounted by gluing the  $ab$  face to the sample holder. Immediately after mounting, crystals were covered with epoxy to avoid water loss. Samples not treated in this way were observed to lose crystallinity with consequent appearance of severe line broadening in the NMR experiments. With this mounting, the three orthogonal rotation axes used in the NMR experiments are  $a$ ,  $b$ , and  $c^*$ . GAL (trihydrate) grew as needles in the orthorhombic group,  $P2_12_12_1$ , with lattice dimensions equivalent to those previously reported<sup>13</sup> and morphological edges along the crystallographic  $a$ ,  $b$ , and  $c$  axes.

In the  $^2\text{H}$  NMR single-crystal experiments described here, electric field gradient tensors,  $V_{ij}$ , are determined from spectra obtained from a crystal sequentially rotated about three orthogonal axes, ( $a$ ,  $b$ ,  $c^*$ ) for GGV or ( $a$ ,  $b$ ,  $c$ ) for GAL. Doublet frequencies were measured for each goniometer angle,  $\phi$ , and least-squares fit to the equation  $a + b \cos(2\phi) + c \sin(2\phi)$ . With these rotation axes and space groups, the frequency versus goniometer angle curves from symmetry-related

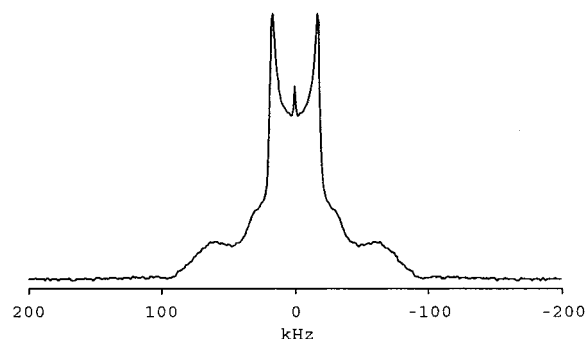


Figure 1.  $^2\text{H}$  NMR powder spectra of GGV.

deuteron pairs are easy to identify; they cross at  $0^\circ$  and  $90^\circ$  and, when viewed together, have a symmetric appearance about  $90^\circ$  (see Figure 3) for the  $a$  and  $c^*$  (or  $c$ ) rotation axes. This allows immediate observation of the expected crystallographic symmetry and confirmation of sample quality. If, for example, GGV is rotated about the  $a$  axis, the components  $V_{c^*c^*} = (a + b)/2$ ,  $V_{bb} = (a - b)/2$ , and  $\pm V_{bc^*} = c$  are determined for a symmetry-related pair. Small errors in crystal alignments yielding small errors in the tensor components are mitigated by averaging the magnitudes of the components for a symmetry-related pair. The accuracy of this approach was confirmed by duplicate GGV single-crystal experiments. Results from two individuals performing the NMR experiments on separately grown single crystals produced quadrupole couplings within 1 kHz and tensor orientations within  $3^\circ$ .

Complete tensors from the three rotations for a symmetry-related pair cannot be uniquely constructed since the frequencies coincide at  $0^\circ$  and  $90^\circ$  goniometer angles. In addition, since frequencies are measured from symmetric doublets, the overall sign of the tensor, i.e., the sign of  $qcc$ , is not determined. Overall sign aside, two possible pairs of tensors can be constructed from the GGV data:

$$\mathbf{V}_+^{(a)} = \begin{pmatrix} V_{aa} & +V_{ab} & V_{ac^*} \\ +V_{ab} & V_{bb} & +V_{bc^*} \\ V_{ac^*} & +V_{bc^*} & V_{c^*c^*} \end{pmatrix}, \quad \mathbf{V}_-^{(a)} = \begin{pmatrix} V_{aa} & -V_{ab} & V_{ac^*} \\ -V_{ab} & V_{bb} & -V_{bc^*} \\ V_{ac^*} & -V_{bc^*} & V_{c^*c^*} \end{pmatrix}$$

$$\mathbf{V}_+^{(b)} = \begin{pmatrix} V_{aa} & +V_{ab} & V_{ac^*} \\ +V_{ab} & V_{bb} & +V_{bc^*} \\ V_{ac^*} & +V_{bc^*} & V_{c^*c^*} \end{pmatrix}, \quad \mathbf{V}_-^{(b)} = \begin{pmatrix} V_{aa} & -V_{ab} & V_{ac^*} \\ -V_{ab} & V_{bb} & -V_{bc^*} \\ V_{ac^*} & -V_{bc^*} & V_{c^*c^*} \end{pmatrix}$$

Tensors  $\mathbf{V}_+^{(a)}$  (or  $\mathbf{V}_+^{(b)}$ ) have the same eigenvalues and their orientations are related by crystal symmetry. In general, eigenvalues of  $\mathbf{V}_\pm^{(a)}$  and  $\mathbf{V}_\pm^{(b)}$  are different and this feature is used to select the correct pair since the eigenvalues or principal components are either approximately known or determined from the powder patterns. In cases where eigenvalues of  $\mathbf{V}_\pm^{(a)}$  and  $\mathbf{V}_\pm^{(b)}$  are similar, we have used approximate knowledge of molecular orientation to select the correct pair.

Once the tensor is determined, the coupling is defined as  $qcc$  (kHz)  $= 4/3 V_{zz}^p$  and the asymmetry as  $\eta = (V_{xx}^p - V_{yy}^p)/V_{zz}^p$  with components labeled according to the convention  $|V_{zz}^p| > |V_{yy}^p| > |V_{xx}^p|$ . The eigenvectors for symmetry-related, magnetically nonequivalent tensors are related by changing the sign of  $y$  for GGV and the signs of  $x$ ,  $y$ , or  $z$  for GAL.

Differential scanning calorimetry (DSC) and thermogravimetric (TGA) analyses were carried out on TA instruments using standard procedures and freshly crystallized samples contained in sealed vessels prior to the experiment. DSC thermograms were scanned at rates varying from 0.5 to  $10^\circ/\text{min}$  with essentially the same results.

## Results

The room-temperature  $^2\text{H}$  NMR powder pattern of GGV is shown in Figure 1, representative room-temperature single-crystal spectra are shown in Figure 2, and the line frequencies

(13) Chaturvedi, S.; Go, K.; Parthasarathy, R. *Biopolymers* **1991**, *31*, 397–407.

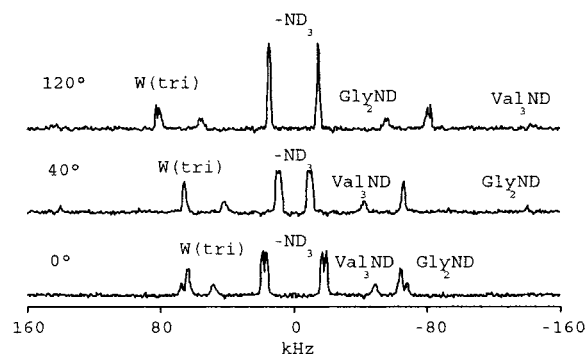


**Figure 2.** Single-crystal  $^2\text{H}$  NMR spectra of GGv for selected orientations.

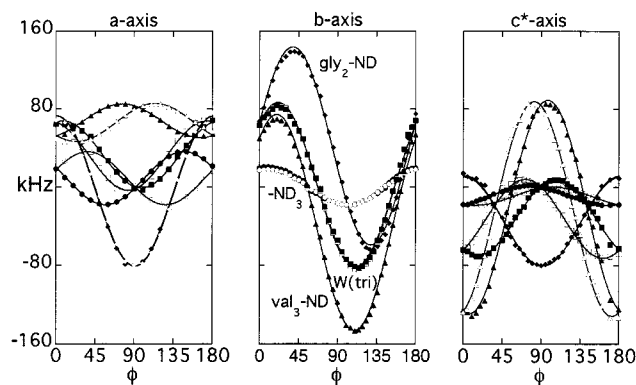


**Figure 3.**  $^2\text{H}$  NMR doublet frequencies as a function of crystal orientation for GGv at room temperature. Frequencies for crystal rotation about the three orthogonal crystallographic axes,  $a$ ,  $b$ , and  $c^*$  are shown. For simplicity, only one of the symmetrically disposed doublet frequencies is graphed.

from many such spectra obtained by systematically rotating a crystal about the  $a$ ,  $b$ , and  $c^*$  axes are shown in Figure 3. The single-crystal data are in complete accord with expectations based on the crystallographic space group<sup>12</sup> as follows: In GGv, there are two magnetically nonequivalent molecules per unit cell related by the 2-fold screw axis,  $b$ . Thus, for orientations in which the crystallographic  $b$  axis is perpendicular to the applied magnetic field (Figure 3b) molecular projections onto the applied magnetic field for the two symmetry-related molecules are equivalent and give equivalent  $^2\text{H}$  NMR spectra. For the  $a$  and  $c^*$  rotations, the number of NMR lines is doubled. Also, curves for lines in the  $a$  and  $c^*$  rotations come in symmetry-related pairs (shown in solid and filled figures) with the same amplitude and average frequency but symmetrically disposed about  $90^\circ$ . Small but noticeable deviations from these symmetries in the rotation graphs arise from small errors in crystal mounting and were mitigated as discussed in the previous section.

In GAL, there are four molecules per orthorhombic unit cell,<sup>13</sup> which reduces to two pairs of magnetically nonequivalent symmetry-related NMR signals per site if the sample is rotated about any of the crystallographic axes; a feature that was experimentally observed (rotation patterns not shown). These data all indicate the possibility of molecular dynamics processes such as water molecule and ammonium ion reorientation which exchange average two or three deuterons to magnetic equivalence. First, the powder spectrum (Figure 1) is dominated by an intense pattern with a residual quadrupole coupling of  $q_{cc} = 49.5$  kHz that is small compared to that for stationary deuterons ( $q_{cc} \sim 200$  kHz).

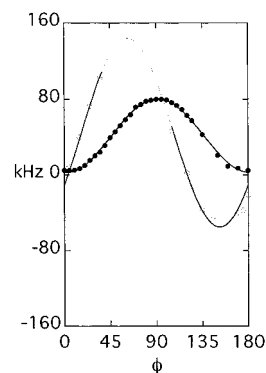


**Figure 4.**  $^2\text{H}$  NMR doublet frequencies as a function of crystal orientation for W(tet) of GGv ( $a$ ,  $b$  axes) at  $-65^\circ\text{C}$ . For simplicity, only one of the symmetrically disposed doublet frequencies is graphed.

Moreover, neglecting the small frequency differences due to crystal misalignment, only four distinct deuterons are observed in the  $b$  axis data or four symmetry-related pairs for the  $a$  and  $c^*$  rotations. GGv potentially shows up to 9 doublets (or tensors) for the  $b$  (or 18 for the  $a$  and  $c^*$ ) axis rotation(s) as follows: 3 from the acid form of the  $\alpha$ -amino group, 2 each from the 2 waters, and 1 each from the Gly<sub>2</sub> and Val<sub>3</sub> amide groups. Clearly, the appearance of both a reduced number of doublets and reduced quadrupole splittings in the powder patterns confirms the presence of substantial dynamic disorder in the exchangeable hydrogen sites. Single-crystal experiments (GGv) at  $-65^\circ\text{C}$  show the loss of the NMR signal for one of the sites for all crystal orientations, a second site is lost for selected orientations, and a new site is observed for all orientations in the  $a$  axis rotation and selected orientations in the  $b$  axis rotation (Figure 4). The new site is seen in only a narrow range of goniometer angles in the  $c^*$  axis rotation (not shown).

Assignment of the observed  $^2\text{H}$  NMR lines to specific deuterons or groups of deuterons is made by examining the magnitudes and vector orientations of the experimentally determined tensor principle components (Table 1) and by comparison with various references vectors calculated directly from the X-ray structure (Table 2). The Gly<sub>2</sub> and Val<sub>3</sub> amide deuterons of GGv are expected to have large quadrupole couplings ( $\sim 200$  kHz) characteristic of stationary amide groups.<sup>14</sup> These two deuterons are assigned to the NMR lines with the largest quadrupole frequencies. These correspond to tensors with  $q_{cc} = 191.5(8)$  kHz,  $\eta = 0.20(1)$  and  $q_{cc} = 203(2)$ ,  $\eta = 0.08(2)$ . These are assigned according to the expectation that the large principal component,  $e_z$ , is approximately along the N– $^2\text{H}$  bond.<sup>14</sup> Angular differences between tensor principal component axis and the expected molecular vectors are listed in Table 2. Given the accuracy of X-ray H-atom coordinates and the approximate nature of the expectation, the assignment is unambiguous. The smaller value of  $q_{cc} = 191.5(8)$  kHz for Gly<sub>2</sub> and its somewhat poorer correlation with the expected orientation of  $e_z$  (Table 2) indicates a degree of librational motion in the center of this peptide. Note also that the components approximately normal to the peptide plane are different for the two amides.

Amide deuteron NMR signals in GGv have orientation-dependent line widths that are generally wider than  $^2\text{H}$  NMR

(14) Usha, M. G.; Peticolas, W. L.; Wittebort, R. J. *Biochemistry* **1991**, *30*, 3955–3962.

**Table 1.** Magnitudes, Asymmetries, and Orientations of  $^2\text{H}$  Electric Field Gradient Tensors<sup>a</sup>

peptide	site	qcc	$\eta$	$e_x$	$e_y$	$e_z$
GGV	$\alpha\text{-N}^2\text{H}_3$	49.2(7)	0.01(3)			0.144, 0.559, 0.817
	Gly <sub>2</sub> N <sup>2</sup> H	192(1)	0.15(1)	0.787, -0.176, -0.591	0.138, 0.984, -0.109	0.601, 0.005, 0.709
	Val <sub>3</sub> N <sup>2</sup> H	208(2)	0.07(2)	0.339, -0.066, 0.939	-0.104, 0.989, 0.107	0.935, 0.134, -0.328
	W(tet) <sup>b</sup>	189(2)	0.30(1)	0.432, 0.307, 0.848	-0.248, 0.945, -0.216	0.867, 0.117, -0.484
	W(tri)	120(1)	0.87(7)	0.260, -0.963, -0.072	0.319, 0.015, 0.948	-0.911, -0.269, 0.311
GAL	$\alpha\text{-N}^2\text{H}_3$	48.5(9)	0.24(3)	0.723, 0.235, -0.650	0.659, -0.515, 0.548	0.206, 0.825, -0.530
	W(tri)	118(2)	0.98(4)	0.164, -0.383, 0.909	-0.985, -0.008, 0.174	0.059, 0.924, 0.378

<sup>a</sup> Vector orientations,  $e_i$ , of component  $V_{ii}$  are in the orthogonal crystal frame ( $a, b, c^*$ ) for GGV or ( $a, b, c$ ) for GAL. <sup>b</sup> Determined at  $-65^\circ\text{C}$ .

**Table 2.** Reference Vectors from the X-ray Structures of GGV and GAL, the Experimental Vectors to Which They Are Compared in the Text, and the Angle,  $\theta$ , between Them

peptide	ref vector	$x, y, z$	exp vector	$\theta^\circ$
GGV	Gly <sub>1</sub> C <sup>α</sup> N	0.181, 0.595, 0.783	$e_z$ $\alpha\text{-N}^2\text{H}_3$	3
	Gly <sub>2</sub> N <sup>2</sup> H	0.851, 0.006, 0.525	$e_z$ Gly <sub>2</sub> N <sup>-2</sup> H	21
	Gly <sub>2</sub> C <sup>α</sup> NC' plane	0.262, 0.926, -0.271	$e_y$ Gly <sub>2</sub> N <sup>-2</sup> H	12
	Val <sub>3</sub> N <sup>2</sup> H	0.928, 0.308, -0.209	$e_z$ Val <sub>3</sub> N <sup>-2</sup> H	12
	Val <sub>3</sub> C <sup>α</sup> NC' plane	0.244, -0.172, 0.954	$e_x$ Val <sub>3</sub> N <sup>-2</sup> H	8
	W(tri) 2-fold	0.136, -0.984, 0.118	$e_x$ W(trig)	14
	W(tri) plane	-0.905, -0.075, 0.419	$e_z$ W(trig)	14
	W(tet) OH	0.933, 0.032, -0.359	$e_z$ W(tet)	11
GAL	Gly <sub>1</sub> C <sup>α</sup> N	0.233, 0.799, -0.555	$e_z$ $\alpha\text{-N}^2\text{H}_3$	0
	W(tri) 2-fold	0.173, -0.159, 0.972	$e_x$ W(trig)	13
	W(tri) plane	-0.985, -0.052, 0.167	$e_y$ W(trig)	1
	W'(tri) 2-fold	-0.439, 0.596, -0.673		
	W'(tri) plane	0.293, 0.803, 0.519		
	W(tet) 2-fold	0.663, 0.684, 0.306		
	W(tet) plane	-0.741, 0.657, 0.136		

signals from the hydrate or  $\alpha$ -amino group. When the quadrupolar splitting is large (Figure 2), i.e., when the N<sup>-2</sup>H bond is parallel to the applied field, the line width is also large. For a small number of orientations, the line is split into the 1:1:1 triplet due to the  $\omega_d/2\pi \sim 1.5$  kHz dipolar coupling with spin 1  $^{14}\text{N}$ . However, for most orientations, only broadening and signal intensity reduction is observed. Moreover, in GAL, amide deuteron NMR signals are not observed in sufficient numbers of orientations to determine assignable tensors. When observed, these signals broadened beyond recognition for small changes in the goniometer setting. A closely related effect was reported for  $^{14}\text{N}$ -coupled  $^{13}\text{C}$  spectra of gramicidin. Resolved  $^{14}\text{N}$ - $^{13}\text{C}$  couplings, apparent in dehydrated samples, were not observed in the hydrated sample, presumably due to self-decoupling<sup>15</sup> which occurs when  $1/T_1(^{14}\text{N}) \gg \omega_d \sim 1 \times 10^4 \text{ s}^{-1}$ .<sup>16</sup> The  $^{14}\text{N}$  relaxation rate is readily estimated on the basis of  $1/T_1(^2\text{H})$  for amides since both nuclei are relaxed by the same spin interaction (quadrupole coupling) undergoing the same dynamics (amide group reorientation). Consequently, their relaxation rates are proportional to the squares of their respective quadrupole coupling constants; 200 kHz for  $^2\text{H}$  and 3.2 MHz for  $^{14}\text{N}$ .<sup>17</sup> Based on  $1/T_1(^2\text{H}) \sim 20 \text{ s}^{-1}$  for amides in GGV, we estimate  $1/T_1 \sim 5 \times 10^3 \text{ s}^{-1}$  for  $^{14}\text{N}$ ; a value comparable to  $\omega_d$  in which case broadening<sup>16</sup> of the  $^2\text{H}$  spectrum is expected as observed. We anticipate that this effect is even more evident in GAL where amide signals are difficult to observe.

The remaining tensors observed at room temperature for both GGV and GAL, are from solvate waters and the  $\alpha$ -amino groups. For these sites, quadrupolar couplings are reduced from

the static values and are thus motionally averaged. The smallest tensor found for GGV and for GAL have qcc = 49.2 and 48.5 kHz, respectively. These are characteristic of protonated  $\alpha$ -amino groups undergoing rapid 3-fold reorientation about the Gly<sub>1</sub> C<sup>α</sup>-N bond. These assignments are confirmed in both peptides by noting that  $e_z$  (Table 1), the direction of the symmetry axis of the averaged tensor, is coincident with the direction of the Gly<sub>1</sub> C<sup>α</sup>-N bond (Table 2). Note that this is realized with excellent accuracy (within  $3^\circ$  for GGV and  $0^\circ$  for GAL) since the tensor component direction is determined by the motion and the X-ray coordinates are for heavy atoms. Also, the excellent correlation of tensor component orientation with X-ray structure indicates the accuracy of the single-crystal NMR measurements.

As a consequence of the above, only one tensor at room temperature is attributable to one of the two waters in GGV or one of the three waters in GAL. For both peptides, the observed water has qcc  $\sim 118$  kHz and  $\eta \sim 1$ , values characteristic of solvate waters undergoing fast  $180^\circ$  flips about the molecular 2-fold axis.<sup>5</sup> For this motion, the directions of the tensor principal components with large and small magnitude are along the water molecular plane and 2-fold axis, respectively. In this work, we do not determine the absolute sign of qcc, and since  $\eta$  is very close to 1, the largest component direction can reasonably be taken as either  $e_y$  or  $e_z$  when searching for a correlation between tensor orientation and molecular structure. Since solvate H-atoms were not reported for GGV,<sup>12</sup> reference vectors for solvate listed in Table 2 are calculated using the heavy atom positions for the proposed H-bond acceptors.

Figures 5 (GGV) and 6 (GAL) show the proposed water H-bond arrangements. To show all relevant structural features, two complete molecules (two turns of the helix) are included as well as relevant additional N-terminal  $\alpha$ -amino group and C-terminal carboxylate group from neighboring molecules.<sup>12,13</sup> Common to both structures are waters with three and four H-bonds. Acceptors for W(tri) are the C-terminal carboxylate and Gly<sub>1</sub> C'=O and the single donor is a protonated  $\alpha$ -amino group. Acceptors and donors for W(tet) are symmetry-related carboxylates and protonated  $\alpha$ -amino groups, respectively. It bridges adjacent peptides along the helix axis. A second trigonally coordinated water, W'(tri), is unique to the GAL structure.

For both GGV and GAL, the only acceptable correlation between the water tensor orientations (Table 1) and the H-bonding structure (Table 2) is with W(tri).

The tetrahedrally coordinated water in both peptides does not yield an observable  $^2\text{H}$  signal at room temperature. A well-demonstrated feature of the  $^2\text{H}$  NMR experiment is that if deuterons undergo structural dynamics at a rate comparable to the quadrupole frequencies; they are essentially unobservable due to severe broadening and attenuation of the solid echo

(15) Wang, C.; Teng Q.; Cross, T. A. *Biophys. J.* **1992**, *61*, 1550–1556.

(16) Abragam, A. *The Principles of Nuclear Magnetism*; Oxford University: London, 1961.

(17) Rabbani, S. R.; Edmonds, D. T.; Gosling, P.; Palmer, M. H. *J. Magn. Reson.* **1987**, *72*, 230–237.

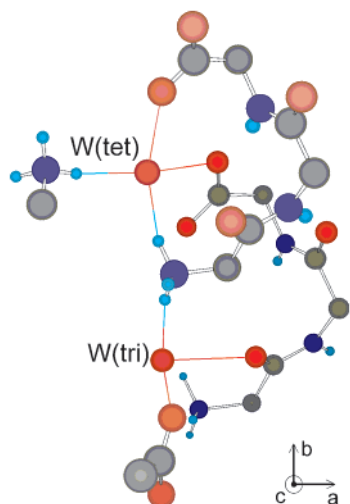


**Figure 5.** X-ray structure of GGv.<sup>12</sup> In order that relevant details for the water H-bonds are shown, the figure includes two complete molecules, an N-terminal  $\alpha$ -ammonium, and a C-terminal carboxylate. Colored bonds are the H-bonds proposed on the basis of the X-ray structure. In addition to the H-bonds shown, each protonated  $\alpha$ -amino is linked to a second W(tet).

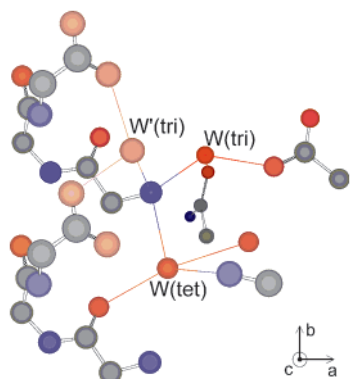


**Figure 6.** X-ray structure of GAL.<sup>13</sup> In order that relevant details for the water H-bonds are shown, the figure includes two complete molecules, a carbonyl, an amide, and a carboxylate group. Colored bonds are the H-bonds proposed on the basis of the X-ray structure.

signal.<sup>18,19</sup> For GGv at  $-65\text{ }^{\circ}\text{C}$ , the  $a$  axis rotation shows the disappearance of the  $\alpha$ -amino signal at all orientations and the W(tri) signal at most orientations (data not shown). Thus, the 3-fold and 2-fold reorientations of these two groups are slowed into the intermediate exchange regime. Also seen, most clearly in the  $-65\text{ }^{\circ}\text{C}$   $a$  axis rotation, is the appearance of a new signal (Figure 4). It is systematically found in most orientations in the  $b$  axis rotation and a small number of orientations in the  $c^*$  axis rotation (not shown). These data are sufficient to determine an approximate tensor with coupling, 189(2) kHz, and asymmetry, 0.30(1). These values approach that for stationary waters and the orientation ( $e_z$ ) is within  $11^{\circ}$  of one O–H vector for the tetrahedral water. With this assignment, we conclude that the tetrahedrally coordinated water is nearly stationary at  $-65\text{ }^{\circ}\text{C}$  and in intermediate exchange at room temperature. By comparison, the 3-coordinate waters move more rapidly; they are in fast exchange at room temperature and intermediate exchange at  $-65\text{ }^{\circ}\text{C}$ .

Previously it was observed that the rotationally mobile waters in  $\beta$ -cyclodextrin $\cdot$ 11H<sub>2</sub>O are also translationally mobile; i.e., waters rapidly move among the different lattice sites and yield a single exchange-averaged <sup>2</sup>H NMR signal. While this rapid

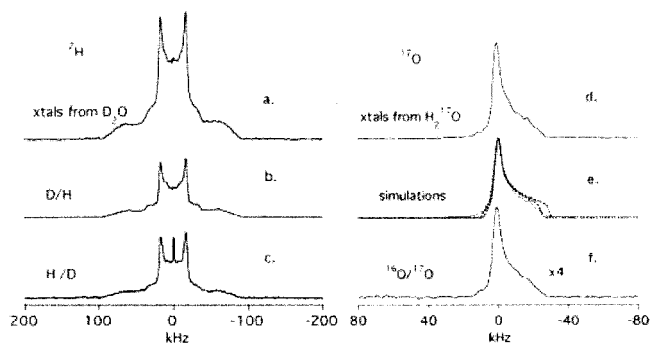


**Figure 7.** Vapor-phase water exchange of crystalline GGv at  $50\text{ }^{\circ}\text{C}$ . (a) <sup>2</sup>H powder spectra of GGv $\cdot$ 2<sup>2</sup>H<sub>2</sub>O after recrystallization from <sup>2</sup>H<sub>2</sub>O and (b) after 10-days exposure to H<sub>2</sub>O vapor. (c) Spectrum obtained after exposure of GGv $\cdot$ 2H<sub>2</sub>O to <sup>2</sup>H<sub>2</sub>O vapor for 10 days. (d) <sup>17</sup>O powder spectrum of GGv $\cdot$ 2H<sub>2</sub><sup>17</sup>O after recrystallization from H<sub>2</sub><sup>17</sup>O and (f) following 8-days exposure of GGv $\cdot$ 2H<sub>2</sub>O to H<sub>2</sub><sup>17</sup>O vapor. (e) <sup>17</sup>O powder pattern simulations (dotted lines) as compared to experiment (solid line). In the simulations,  $qcc = 6.5$  and  $7.1$  MHz and  $\eta = 1$ .

translational motion is clearly not seen here, the possibility of slower translational motion is examined by vapor-phase isotope exchange (Figure 7) using both <sup>2</sup>H and <sup>17</sup>O NMR. Crystalline GGv $\cdot$ 2<sup>2</sup>H<sub>2</sub>O or GGv $\cdot$ 2H<sub>2</sub>O was sealed in a long (2.5 cm) sample tube containing a drop of H<sub>2</sub>O, <sup>2</sup>H<sub>2</sub>O, or H<sub>2</sub><sup>17</sup>O, respectively, at the opposite end. When placed in the NMR probe, the  $\sim$ 0.5-cm end containing the solid peptide is warmed by a stream of gas to  $50\text{ }^{\circ}\text{C}$  to increase the water vapor pressure and minimize condensation on the crystal surfaces. <sup>2</sup>H and <sup>17</sup>O spectra of samples grown from the <sup>2</sup>H- and <sup>17</sup>O-labeled water, respectively, are shown in Figure 7a,d.

After 10-days exposure of GGv $\cdot$ 2<sup>2</sup>H<sub>2</sub>O to H<sub>2</sub>O (Figure 7b), a more than 2-fold decrease in the powder NMR signal is observed. In the reverse experiment (Figure 7c), exposure of solid GGv $\cdot$ 2H<sub>2</sub>O to <sup>2</sup>H<sub>2</sub>O vapor for the same period results in the appearance of the characteristic GGv <sup>2</sup>H NMR spectrum. Importantly, <sup>2</sup>H signals corresponding to the hydrate (contained in the broad shoulder) and to the  $\alpha$ -amino group (the narrower, more intense doublet pattern) both appear, indicating the presence of proton transfer. The <sup>17</sup>O exchange experiment, wherein the appearance of a signal indicates diffusion of water in the crystal lattice, shows that after 8 days  $\sim$ 25% exchange has occurred (Figure 7f). Moreover, the <sup>17</sup>O quadrupole coupling of the exchange-labeled sample (Figure 7f) is identical to that from the fully labeled material (Figure 7d). The quadrupole coupling has a value in the range of 6.5–7.1 MHz (Figure 7e), which is comparable to that expected for strongly H-bonded waters. Note that the 2-fold flip motion identified by <sup>2</sup>H spectroscopy does not average the <sup>17</sup>O tensor since one of the tensor principle components is coincident with the 2-fold axis. Although rather slow, these experiments confirm the presence of translational mobility of both protons and water in the GGv lattice.

Samples of the crystalline GGv and GAL hydrates were examined by TGA and DSC. Weight losses are 14.7% for GGv and 18.0% for GAL, values in excellent agreement with those expected for the loss of two (GGv) or three (GAL) waters. Waters are expelled over a broad, 40 $^{\circ}$  temperature range

(18) Wittebort, R. J.; Olejniczak, E. T.; Griffin, R. G. *J. Chem. Phys.* **1987**, *86*, 5411–5420.

(19) Wittebort, R. J.; Usha, M. G.; Ruben, D. J.; Wemmer, D. E.; Pines, A. *J. Am. Chem. Soc.* **1987**, *110*, 5668–5671.

centered at 90 °C for GGV and 60 °C for GAL. Slowing the DSC scanning rate to 0.5 °C/min did not resolve the endotherm into separate events, indicating that all waters are simultaneously eliminated. The DSC endotherms have molar enthalpies of 106.7 (GGV) and 157 kJ (GAL). These correspond to average molar enthalpies of 53 kJ/water molecule or (based on the X-ray H-bond pattern) 15 kJ/H-bond.

## Discussion

Ordered waters play important roles in protein, protein–ligand, and protein–DNA structures.<sup>1,3,20–23</sup> For example, conserved structural waters are crucial for both lysozyme activity<sup>20</sup> and substrate binding.<sup>21</sup> By filling in gaps between protein and the substrate surfaces and forming H-bond networks, water molecules can affect the specificity of proteins for different substrates.<sup>22</sup> In addition, water-mediated substrate recognition might be a general process in DNA–protein binding.<sup>23</sup> The degree to which waters stabilize these structures is not, however, well understood. For example, waters H-bonded to hydroxyprolyl residues in collagens have long been thought to be a source of structural stabilization.<sup>10</sup> However, the recent discovery of hyperstable synthetic collagen sequences lacking hydroxyproline<sup>24</sup> and disagreements on the amount of ordered water in high-resolution X-ray structure of triple helical peptides<sup>25,26</sup> indicate that water structure in well-defined model systems is worthy of detailed studies. Herein we have examined two peptide hydrates by single-crystal and powder NMR. Without bridging waters in these peptides, the observed conformation could not satisfy expected peptide H-bond interactions; thus, a structural role is indicated for the hydrate.

The DSC and TGA results, interpreted on the basis of the number of H-bonds identified in the X-ray structure, indicate an average molar H-bond energy of –15 kJ or an average water binding enthalpy of –50 kJ/molecule of hydrate. An estimate of the range of H-bond energies in proteins<sup>27</sup> is –12 to –30 kJ. Note that the waters examined in these short, zwitterionic peptides are predominantly H-bonded to charged groups. While these waters are less strongly held than those in inorganic salts and coordination complexes, it is likely that they are representative of the more strongly held waters in proteins. In inorganic complexes, an upper limit of ~8 kJ/mol has been estimated<sup>28</sup> for the unfavorable contribution of water ordering to its free energy. Albeit positive, this value is small compared to the average hydrate enthalpy, 50 kJ/mol, measured here. We conclude that these structural waters make an important thermodynamic contribution to the overall stability of the conformations in GGV and GAL.

Unlike  $\beta$ -cyclodextrin·11H<sub>2</sub>O where the H-bond partners are sugar OH groups, the waters in these peptides appear translationally fixed for times less than 10<sup>–3</sup> s. They do, however, undergo faster (> 10<sup>5</sup> s<sup>–1</sup>) rotations which are experimentally

defined by the magnitudes and orientations of the motionally average <sup>2</sup>H electric field gradient tensors. In both GGV dihydrate and GAL trihydrate, a single water is observed at room temperature by <sup>2</sup>H NMR. It is assigned to the 3-coordinate water, W(tri), in both structures which has carbonyl, carboxylate, and protonated  $\alpha$ -amino H-bond partners. These waters undergo rapid flips ( $\gg 10^5$  s<sup>–1</sup>) about the 2-fold axis at room temperature, and the orientation of their dynamically averaged <sup>2</sup>H electric field gradient tensor is close to that expected based on the proposed H-bonding arrangements in the X-ray structure. The  $\alpha$ -amino groups are also dynamic (rapid 120° flips about the 3-fold axis). Consequently, the three H-bonds stabilizing W(tri) are transient. When GGV is cooled to –65 °C, the NMR signals for this water and the  $\alpha$ -amino group are lost, indicating that the flip rates have slowed to the intermediate exchange regime (10<sup>3</sup>–10<sup>5</sup> s<sup>–1</sup>). Signal loss occurs because intermediate exchange effects result in severe line broadening and <sup>2</sup>H NMR echo signal attenuation.<sup>18,19</sup> Also observed upon cooling is a new NMR signal. This signal is observed for most but not all crystal orientations and has a large splitting ( $q_{cc} = 189$  kHz) indicating that the NMR slow exchange limit (rate < 10<sup>3</sup> s<sup>–1</sup>) is approached; i.e., the deuteron is approximately stationary. On the basis of tensor orientation and that all other deuterons are accounted for, it is assigned to the tetrahedrally coordinated water, W(tet). Consequently, we conclude that W(tet) in GGV is also dynamic at room temperature but moves more slowly (10<sup>3</sup>–10<sup>5</sup> s<sup>–1</sup>) than the 3-coordinate water. The H-bond partners in this case are four charged groups: two carboxylates and two protonated  $\alpha$ -amino groups. It has not been possible to determine an explicit model for the dynamics of W(tet) due to S/N limitations at room temperature. At higher temperatures, where fast-exchange dynamics would likely occur, the water is expelled.

Both the number and charge of the H-bond partners systematically affect hydrate dynamics. This correlates well with the <sup>2</sup>H NMR results. A water with four charged H-bond partners, W(tet) in GGV, moves more slowly than the W(tri), which has two charged and one neutral (carbonyl) partner. Moreover, with the assumption that W'(tri) in GAL is not observed at room temperature for the same reason as W(tet) in GGV (intermediate exchange), then three charged H-bond partners is sufficient to substantially slow internal reorientation.

The possibility of additional hydrate motion that establishes proton transfer in the lattice is indicated by the isotope-exchange experiments. As observed either by disappearance of characteristic NMR signals when GGV·2<sup>2</sup>H<sub>2</sub>O is equilibrated with H<sub>2</sub>O vapor or by their appearance when GGV·2H<sub>2</sub>O is equilibrated with <sup>2</sup>H<sub>2</sub>O, both solvate water and the protonated  $\alpha$ -amino group are extensively labeled. Two ways that deuterons can enter the crystal lattice are by direct diffusion of water into the lattice or by proton exchange at the crystal surface. Direct diffusion of water through a crystal lattice has been confirmed in  $\beta$ -cyclodextrin·11H<sub>2</sub>O<sup>7</sup> and the <sup>17</sup>O exchange experiments show that this occurs in the GGV lattice, albeit on a much longer time scale of days. Proton transfer at the surface remains a possibility. In either case, labeling of both water and  $\alpha$ -amino deuterons requires proton exchange between these groups in the crystal. This is seen in the GGV structure (Figure 5). No direct proton transfer between  $\alpha$ -amino groups (or between waters) can occur without transfer to a bridging water (or  $\alpha$ -amino). H/D ( $D =$

(20) Nagendra, H. G.; Sukumar, N.; Vijayan, M. *Proteins* **1998**, *32*, 229–240.

(21) Maenaka, K.; Matsushima, M.; Song, H.; Sunada, F.; Watanabe, K.; Kumagai, I. *J. Mol. Biol.* **1995**, *247*, 281–293.

(22) Wilson, I. A.; Fremont, D. H. *Semin. Immunol.* **1993**, *5*, 75–80.

(23) Robinson, C. R.; Sligar, S. G. *J. Mol. Biol.* **1993**, *234*, 302–306.

(24) Holmgren, S. K.; Taylor, K. M.; Bretscher, L. E.; Raines, R. T. *Nature* **1998**, *392*, 666.

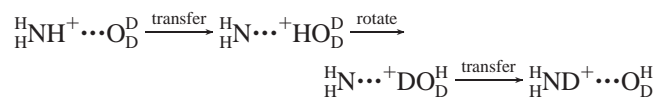
(25) Bella, J.; Brodsky, B.; Berman, H. M. *Structure* **1995**, *3*, 893–906.

(26) Nagarajan, V.; Kamitori, S.; Okuyama, K. *J. Biochem.* **1998**, *124*, 1117–1123.

(27) Voet, D.; Voet, J. G. *Biochemistry*, 2nd ed.; J. Wiley & Sons: New York, 1995; Chapter 7.

(28) Dunitz, J. D. *Science* **1994**, *264*, 670.

$^2\text{H}$ ) exchange is envisioned as follows:



Without reorientation of the hydronium ion about its 3-fold axis, isotope exchange does not occur. This motion occurs in addition to the fast 2-fold flips confirmed for W(tri) on the basis of the averaged  $^2\text{H}$  electric field gradient tensor. Averaging of the  $^2\text{H}$  tensor is unaffected by this motion, as a consequence of an expected low proportion of protonated waters, slow rotation of the hydronium ion ( $< 10^3 \text{ s}^{-1}$ ), or both. Since the GGV lattice contains infinite chains of protonated  $\alpha$ -amino groups bridged by W(tet), this “proton wire” process alone is sufficient to

achieve the observed isotope exchange. Limiting factors contributing to the observed exchange rate of days could be the observed slow diffusion of water into the lattice, slow proton exchange at the crystal surface, low probability of the hydronium ion, or slow reorientation about its 3-fold axis.

**Abbreviations:** GGV, Gly-Gly-Val $\cdot 2\text{H}_2\text{O}$ ; GAL, Gly-Ala-Leu $\cdot 3\text{H}_2\text{O}$ ; D,  $^2\text{H}$ ; qcc, quadrupolar coupling constant;  $\eta$ , asymmetry parameter; NMR, nuclear magnetic resonance; DSC, differential scanning calorimetry; TGA, thermogravimetric analysis.

**Acknowledgment.** We thank Dr. Gene Lamm for helpful discussions.

JA017364R